Quasi-static Motion of Bubbles in Microchannel Contractions

Mads Jakob Jensen, Goran Goranović, and Henrik Bruus

Mikroelektronik Centret (MIC), Technical University of Denmark (DTU), DK-2800 Kgs. Lyngby
mjj@mic.dtu.dk

ABSTRACT

We present a thorough theoretical and computational study of quasi-static motion of bubbles in microfluidic channel contractions. We investigate how geometry and surface physics formulated in terms of surface free energies and contact angles affects the behavior of incompressible bubbles passing through a contraction. The analysis carried out is easily generalized to a variety of channel geometries and channel cross sections.

Keywords: Microchannel contraction, bubble, quasi-static motion, modelling, balancing force.

1 INTRODUCTION

In microchannels gas bubbles present a significant problem: they can block and/or disrupt the flow, and disturb measurements in an uncontrolled manner. For that reason, the sample liquids are usually treated by various methods before they enter a microfluidic chip. However, in spite of such efforts gas bubbles may still be present, and once there it often requires large applied pressures to push them out of the system [1].

In this paper we focus on microchannel contractions as they are often areas where bubble clogging problems arise in microfluidic systems. An analysis of the motion of a bubble through a channel contraction is generally very complicated. If the model is to be complete it requires detailed modelling of the physical processes near the contact lines, e.g., wetting [2], dynamic contact angle [3], and static and dynamic friction [4]. Furthermore, the modelling requires a precise description of the liquid-gas free surface and of course of the dynamics in the bulk fluids.

In this work we will however focus on a simplified model. As a first approach we will investigate the quasi-static motion of an incompressible bubble through a microchannel contraction of spherical cross section. This implies that all dynamic components are neglected, the model basically predicts the behavior of the potential energy of the system. The system remains arbitrarily close to equilibrium at all bubble positions, i.e., the balancing force required to hold the bubble at rest is determined for all positions. It is thus possible to predict the maximal balancing force for a given contraction geometry.

In the following we present the physics used in the numerical models as well as some analytical results used to test the model. The model is then presented together with a discussion of selected results.

2 PHYSICS

The total energy E_{tot} of a bubble passing through a microchannel contraction is the sum of the surface free energy, gravitational energy and kinetic energy. The bubble is assumed to be incompressible, an assumption leading to negligible relative errors smaller than one percent. Furthermore, we study only quasi-static motion of the bubble resulting in zero kinetic energy. Finally, we treat channels of widths less than 300 μm which is significantly smaller than the capillary length Δ_c,

$$\Delta_c = \left(\frac{\sigma_{\text{lg}}}{\rho g}\right)^{\frac{1}{2}} = 3 \times 10^3 \ \mu\text{m}, \tag{1}$$

where σ_{lg} is the liquid-gas surface tension, ρ is the density of the liquid and g the gravitational acceleration. As a result gravitational energies can be neglected.

In conclusion, the total energy of the system is given only by the surface free energy, i.e., the sum of interfacial energies times interfacial areas

$$E_{\text{tot}} = \sum_i \sigma_i A_i = \sigma_{\text{lg}} A_{\text{lg}} + \sigma_{\text{sg}} A_{\text{sg}} + \sigma_{\text{sl}} A_{\text{sl}}. \tag{2}$$

Here σ_{lg}, σ_{sg}, and σ_{sl} is the surface free energy of the liquid-gas, solid-gas, and solid-liquid interface, respectively. Likewise for the areas A_i. The total external force F needed to balance the bubble is given by the gradient of the total energy with respect to the center of mass coordinate of the bubble x_{cm}, hence

$$F = \frac{dE_{\text{tot}}}{dx_{\text{cm}}}. \tag{3}$$

The center of mass may be found as

$$x_{\text{cm}} = \frac{1}{V_{\text{tot}}} \sum_{j=1}^{5} x_j V_j \tag{4}$$

where x_j are the center of mass coordinates of the different volume sections V_j depicted in Fig. 2. The total

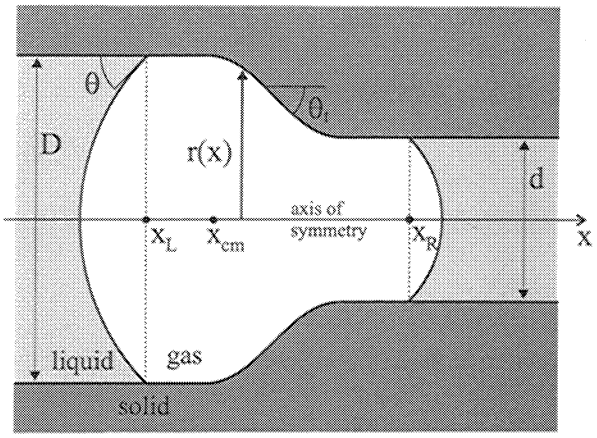

Figure 1: Longitudinal cross section of a 3D channel of circular transverse cross sections. The channel is contracting from diameter D to d. The specific channel profile is defined by the function $r(x)$ and the tapering angle θ_t. The contact angle is denoted θ. The coordinate of the left and right contact lines are $x_{\rm L}$ and $x_{\rm R}$, respectively. The center of mass coordinate of the gas bubble is denoted $x_{\rm cm}$.

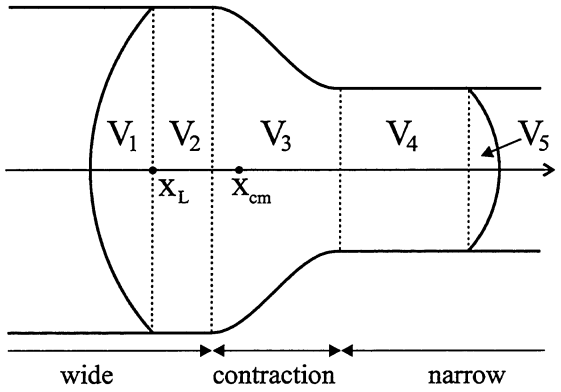

Figure 2: Division of the bubble into the volume parts V_j for $j = 1, 2, 3, 4, 5$. The wide contraction, and narrow parts of the channel are further identified.

volume $V_{\rm tot} = \sum_j V_j$ is constant as the bubble is assumed incompressible.

The bubble is passing from a wide channel of diameter D to a narrow channel of diameter d. The specific shape of the contraction is in the following defined by a function $r(x)$. A so-called tapering angle θ_t is defined at the steepest part of the contraction. All details are presented in Figs. 1 and 2. The channel is of circular cross section hence at equilibrium the liquid-gas interface is part of a sphere.

The bubble is also assumed to wet the solid surface as shown in Fig. 1. There is a contact angle θ at the contact line. The relation between the interfacial free energies and the static contact angle is given by the Young equation,

$$\sigma_{\rm lg} \cos\theta = \sigma_{\rm sg} - \sigma_{\rm sl}. \qquad (5)$$

The relation between curvature and pressure is given by the Young-Laplace equation [5].

2.1 Analytical Work

To be able to test the model discussed in the next section some analytical work is here shortly presented. The total balancing force on a large bubble with the left contact line in the wide channel and the right contact line in the narrow channel ($V_j \neq 0$ for all j, see Fig. 2) is given by,

$$\begin{aligned} \frac{dE_{\rm tot}}{dx_{\rm cm}} &= \frac{dE_{\rm tot}}{dx_{\rm L}} \frac{dx_{\rm L}}{dx_{\rm cm}} \\ &= \sigma_{\rm lg} \cos\theta \pi D^2 \left(\frac{1}{d} - \frac{1}{D}\right) \frac{dx_{\rm L}}{dx_{\rm cm}}. \end{aligned} \qquad (6)$$

To obtain the expression for $\frac{dE_{\rm tot}}{dx_{\rm L}}$ volume conservation has been used. Note that the expression is constant for a given geometry. An expression for $\frac{dx_{\rm L}}{dx_{\rm cm}}$ is also found as

$$\begin{aligned} \frac{dx_{\rm L}}{dx_{\rm cm}} &= \frac{1}{V_{\rm tot}} \left\{ V_1 + \frac{1}{2}\left[V_2 + \left(\frac{D}{d}\right)^2 V_4 \right] \right. \\ &\quad \left. + (x_4 - x_2)\left(\frac{D}{2}\right)^2 \pi + \left(\frac{D}{d}\right)^2 V_5 \right\}, \end{aligned} \qquad (7)$$

where x_2 and x_4 are the center of mass coordinates of the volumes V_2 and V_4, respectively. In Eq. (7) the dependence upon x_L is through V_2, V_4, x_2, and x_4 as V_1 and V_5 are constant for the analyzed bubble configuration.

3 THE MODEL

In order to find the maximal force acting on a bubble for a given geometry a semi-analytical model of the contracting channel is implemented in MatLab. A numerical Romberg integration scheme is used to determine the location of the right contact line $x_{\rm R}$ for a given position of the left contact line $x_{\rm L}$ on Fig. 1. The center of mass coordinate $x_{\rm cm}$ is then determined together with the respective interface areas A_i. For a specific geometry defined through $r(x)$ and the tapering angle θ_t the maximal force is found through Eqs. (2) and (3).

In the specific case discussed in this paper we use PMMA as the solid material, the liquid is water and the gas is air. This configuration has the physical parameters given in Table 1.

The function defining the shape of the contraction $r(x)$ is depicted in Fig. 3 where the corner arc length A_l is defined.

Parameter	Value	Unit
σ_{lg}	72.5×10^{-3}	Jm^{-2}
σ_{sg}	38.9×10^{-3}	Jm^{-2}
σ_{sl}	16.5×10^{-3}	Jm^{-2}
θ	72^o	-

Table 1: Physical parameters for air-water-PMMA configurations Refs. [5,6].

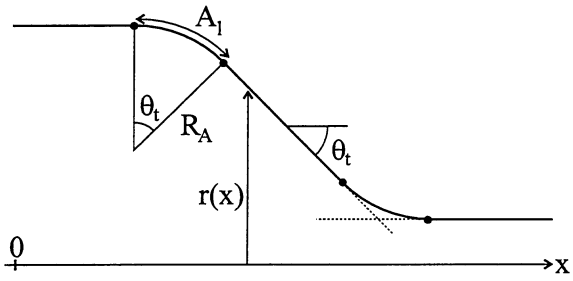

Figure 3: Specific definition of the shape function $r(x)$ defined through the tapering angle θ_t and a corner length A_l. The shape consists of three straight line segments and two circular arcs.

4 RESULTS

To illustrate some of the results obtained the current analysis we restrict the analysis to a few changes in parameters. The geometry is defined with $D = 300$ μm, $d = 150$ μm and the corner length $A_l = 30$ μm. The solid is PMMA, the liquid is water, and the gas is air and only one initial bubble volume is used. The aim of the analysis is to optimize the tapering geometry with respect to the tapering angle θ_t, i.e., find the optimal tapering angle to reduce the force needed to get a bubble through the contraction.

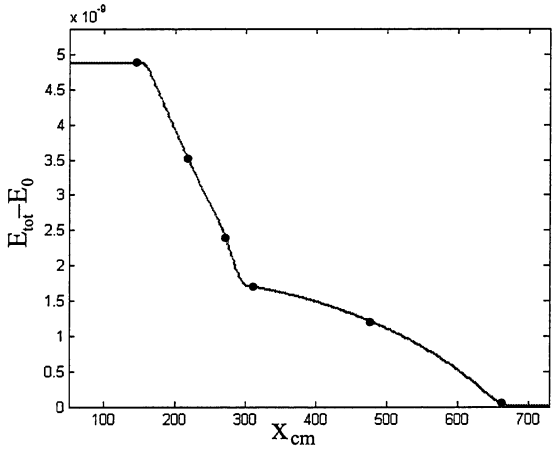

Figure 4: The total energy vs. $x_{\rm cm}$ for $\theta_t = 20^o$.

In Fig. 4 the total free energy of the system is depicted for $\theta_t = 20^o$. A constant zero point energy E_0 has been subtracted. In Fig. 5 the corresponding balancing force F given by Eq. (3) is plotted as a function of $x_{\rm cm}$. The force is always negative meaning that the bubble is pulled towards the narrow segment.

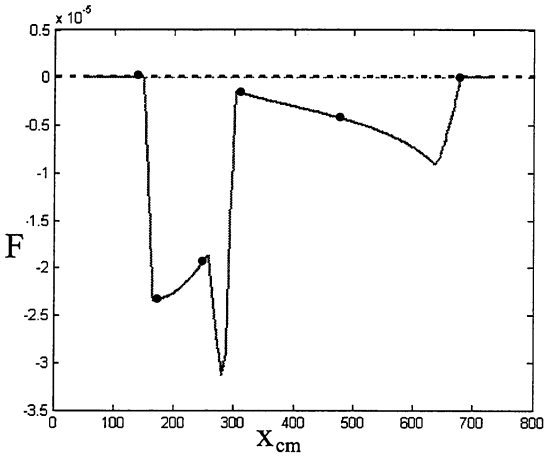

Figure 5: Balancing force F vs. $x_{\rm cm}$ for $\theta_t = 20^o$.

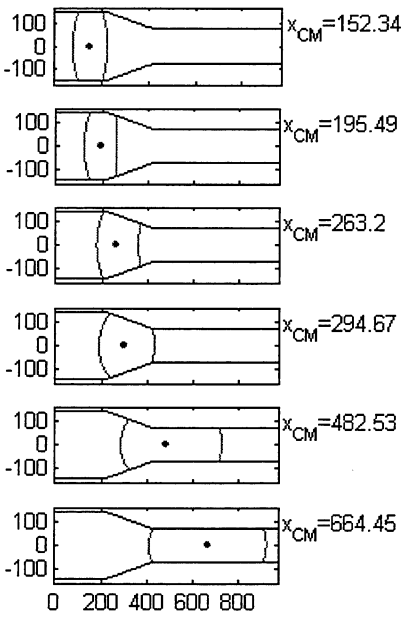

Figure 6: Bubble position in the channel geometry used in Figs. 4 and 5 for six different center of mass coordinates.

Fig. 6 shows the bubble at six different positions, these positions are marked on Figs. 4 and 5 with small dots.

In Figs. 7 and 8 the tapering angle is changed from 20^o to 33^o. For 230 μm $< x_{\rm cm} <$ 290 μm the force is positive meaning that there is a potential energy barrier.

In the spirit of the previously discussed results Fig. 9 depicts the maximal force for a given channel configura-

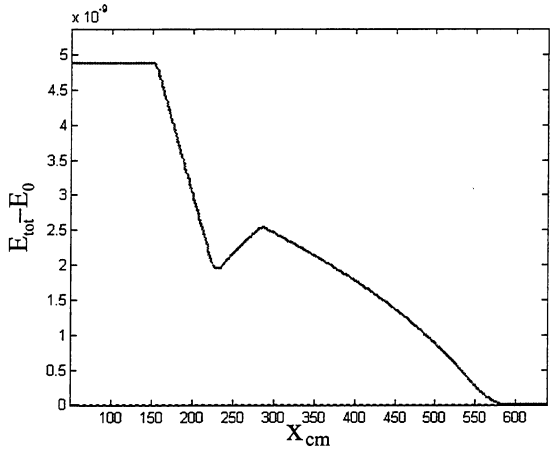

Figure 7: The total energy vs. $x_{\rm cm}$ for $\theta_t = 33^o$.

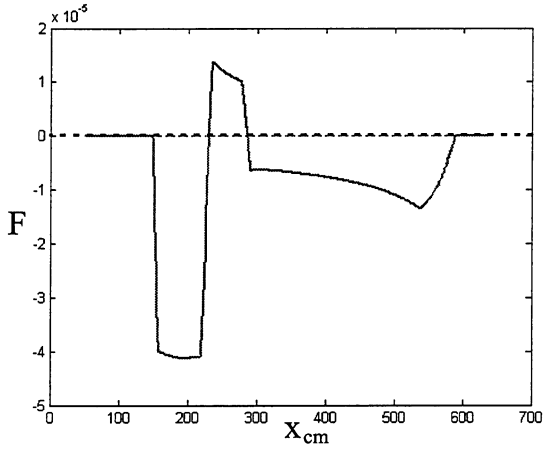

Figure 8: Balancing force F vs. $x_{\rm cm}$ for $\theta_t = 33^o$.

tion defined by the tapering angle θ_t. The graph clearly shows that some tapering angles ease the passage of bubbles. An optimal tapering angle window is present for the interval $14^o < \theta_t < 23^o$ for the geometrical configuration defined by D, d, and A_l. For angles greater than about 24^o the maximal force is seen to increase dramatically. This transition corresponds to a configuration where the bubble can span the entire contraction region ($V_j \neq 0$ for all j see Fig. 2). In this regime the theoretical results obtained in Eqs. (6) and (7) have been compared to the numerical results and are seen to concorde.

5 CONCLUSION

The effects of geometry on the quasi-static motion of bubbles through a microchannel contraction are modelled. It is illustrated that an optimal design may be found for a specific geometry. The method used is very general and may be extended to other geometries. The model may also be extended to include wetting layers as used in Ref. [7] or may be used fore pore modelling as in Ref. [8].

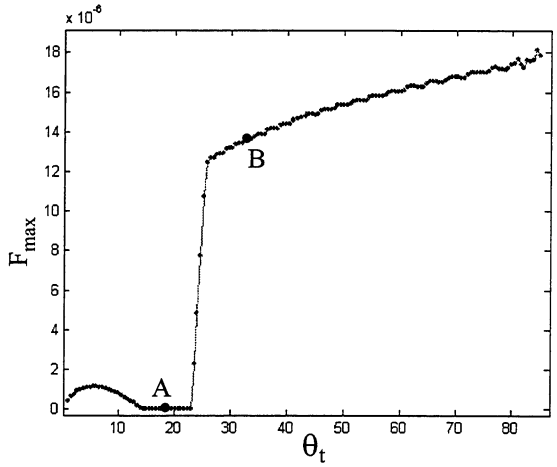

Figure 9: The maximal balancing force as a function of the tapering angle θ_t. Detailed pictures of the situation at the point A is given in Figs. 4 and 5 and for the point B in Figs. 7 and 8.

6 ACKNOWLEDGEMENT

We are grateful to Peter Gravesen, Danfoss, for his inspiring discussions at an early stage. This work is partly supported by the Danish Technical Research Council, μTAS Frame Program Grant No. 9901288.

REFERENCES

[1] P. Gravesen, J. Branebjerg, and O. Søndergård Jensen, J. Micromech Microeng., **3**, 168 (1993).

[2] P. G. de Gennes, "Wetting: statics and dynamics", Rev. of Mod. Phys. **57**, 827-862 (1985).

[3] L. M. Pismen, B. Y. Rubinstein, "Kinetic Slip Condition, van der Waals Forces, and Dynamic Contact Angle", Langmuir **17**, 5265- 5270 (2001).

[4] M. A. Tenan, S. Hackwood, and G. Beni, "Friction in capillary systems", J. Appl. Phys **53**, (1982).

[5] A. W. Adamson and A. P. Gast, "Physical Chemistry of surfaces", Sixth Edition, John Wiley and Sons, Inc. 1997.

[6] B. Jańczuk, T. Bialopiotrowicz, and A. Zdziennicka, J. of Colloid and Interface Science **211**, 96-103 (1999).

[7] J. Bico and D. Qur, "Self-propelling slugs in a tube", J. Fluid Mech., **467**, 101-127 (2002).

[8] F. F. Zha, A. G. Fane, C. J. D. Fall, and R. W. Schofield, "Critical displacement pressure of a supported liquid membrane", J. of Membrane Science **75**, 69-80 (1992).